COMMUNICATION

B-MWW Zeolite: The Case Against Single-Site Catalysis

Natalie R. Altvater‡[a], Rick W. Dorn‡[b][c], Melissa C. Cendejas‡[d], William P. McDermott[d], Brijith Thomas[b], Aaron J. Rossini*[b][c], Ive Hermans*[a][d]

Abstract: Boron-containing materials have recently been identified as highly selective catalysts for the oxidative dehydrogenation (ODH) of alkanes to olefins. It has previously been demonstrated by several spectroscopic characterization techniques that the surface of these boron-containing ODH catalysts oxidize and hydrolyze under reaction conditions, forming an amorphous $B_2(OH)_{2x}O_{(3-x)}$ (x = 0 - 3) layer. Yet, the precise nature of the active site(s) remains elusive. In this communication, we provide a detailed characterization of zeolite MCM-22 isomorphously substituted with boron (B-MWW). Using ^{11}B solid-state NMR spectroscopy, we show that the majority of boron species in B-MWW exist as isolated BO_3 units, fully incorporated into the zeolite framework. However, this material shows no catalytic activity for ODH of propane to propene. The catalytic inactivity of B-MWW for ODH of propane falsifies the hypothesis that site-isolated BO_3 units are the active site in boron-based catalysts. This observation is at odds with other traditionally studied catalysts like vanadium-based catalysts and provides an important piece of the mechanistic puzzle.

Zeolites, microporous, crystalline materials composed of characteristic SiO_4 tetrahedra, are among the most widely used industrial catalysts.[1] The so-called T-sites may be replaced with different atoms *via* isomorphous substitution to tune the catalytic properties by - for example - altering the Bronsted/Lewis acidity or creating a catalytic center. Isomorphous substitution can be achieved directly via hydrothermal synthesis or post-synthetically by methods, including impregnation and ion-exchange.[2,3] Although widely applied in industry, isomorphously substituted zeolites are still the subject of many ongoing studies.[4]

Boron-containing materials, such as hexagonal boron nitride and boron nitride nanotubes, have been shown to be highly selective catalysts for the transformation of light alkanes to olefins *via* oxidative dehydrogenation (ODH).[5-11] Analysis of these materials after catalytic testing for the ODH of propane revealed the formation of an oxidized, amorphous boron phase at the catalyst surface. This layer consists of three-coordinate boron with varying numbers of hydroxyl and bridging oxide groups represented by the general formula $B_2(OH)_{2x}O_{(3-x)}$ (x = 0 - 3).[12] To understand the function of this oxidized boron phase, we recently investigated silica-supported boron oxide (B/SiO_2) materials, which showed a similar conversion-selectivity trend and product distribution to the bulk boron-containing catalysts.[13] While these results confirm that the active site is most likely contained in the oxidized boron phase, the precise reaction mechanism and active site structure have not been identified. Magic angle spinning (MAS) ^{11}B solid-state NMR spectroscopy (SSNMR) analysis of the B/SiO_2 materials revealed the $B_2(OH)_{2x}O_{3-x}$ phase restructures under ODH reaction conditions to give a higher degree of boron agglomeration. The observed restructuring is in line with a recent computational study on h-BN that predicts the formation of a highly dynamic oxidized boron active phase under reaction conditions (~500 °C), in agreement with the low Taman temperature of boron oxides.[14]

The large distribution of boron sites in active materials and their dynamic nature under reaction conditions precludes the precise experimental identification of the active site(s). To understand the requirements for active site formation, the synthesis of a material with more controlled, uniform boron oxide speciation is necessary. In this contribution, we focus on zeolite MCM-22 isomorphously substituted with boron (referred to as B-MWW). MWW is an industrially prepared catalysts used as an additive to ZSM-5 for catalytic cracking, in Mobil's Badger Cumene process for the alkylation of benzene, the alkylation of toluene, and the liquid phase epoxidation of propylene.[15-18] The borosilicate form of MWW (also called ERB-1) is used primarily as an intermediate for creating high Si/Al ratio frameworks and for the post-synthetic incorporation of metals into the structure.[19] Because of its industrial applications, we know that the MWW framework can accommodate propylene molecules and is therefore viable for use as a potential propane ODH catalyst.

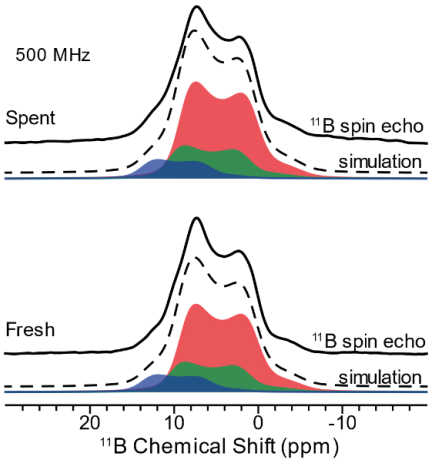

Figure 1. 1D ^{11}B MAS SSNMR spectra of (lower) fresh and (upper) spent B-MWW. The solid lines correspond to the experimental spectra and the dashed lines correspond to analytical simulations. The analytical simulations of fresh and spent B-MWW were generated from parameters reported in Table 1.

[a] N.R. Altvater, Prof. Dr. I. Hermans
Department of Chemical and Biological Engineering
University of Madison – Wisconsin
1415 Engineering Drive, Madison, Wisconsin 53706, USA
E-mail: hermans@chem.wisc.edu
[b] R.W. Dorn, Dr. B. Thomas and Prof. Dr. A.J. Rossini
Department of Chemistry
Iowa State University
2438 Pammel Dr., Ames, IA 50011, USA
Email: arossini@iastate.edu
[c] R.W. Dorn and Prof. Dr. A.J. Rossini
U.S. Department of Energy
Ames Laboratory
311 Iowa State University, Ames, IA 50011, USA
[d] M.C. Cendejas, W.P. McDermott, and Prof. Dr. I. Hermans
Department of Chemistry
University of Wisconsin – Madison
1101 University Avenue, Madison, WI, 53706 USA

‡ These authors contributed equally to this work.
Supporting information for this article is given via a link at the end of the document.

B-MWW was hydrothermally synthesized according to an established literature procedure (see Supporting Information).[20] The successful synthesis of the MWW framework was confirmed by powder X-ray diffraction (Figure S1) and N_2 physisorption (S_{BET} = 498 m^2/g).[20,21] The boron loading was quantified by inductively coupled plasma-mass spectrometry (ICP-MS) to be 1.1 ± 0.1 wt. %. This loading is within the 0.23-2.20 wt. % range for B/SiO_2 catalysts made by incipient wetness impregnation that all showed significant conversion under our ODH reaction conditions.[13]

Table 1. Isotropic chemical shift and electric field gradient tensors for the three site analytical simulations of B-MWW in Figure 1.[a]

Site	δ_{iso} (ppm)	C_Q (MHz)	η	Integration (%)
red	11	2.6	0.0	66
green	12	2.4	0.0	23
blue	15	2.7	0.0	11

[a] Fresh and spent B-MWW were fit to identical parameters.

Catalytic testing for the ODH of propane was performed at 500 °C under a flow of C_3H_8, O_2, and N_2 with a pretreatment at 525 °C under the same gas composition.[13] Surprisingly, the B-MWW material showed no conversion above the background observed with a blank reactor (*i.e.* < 0.5% conversion). This result was unexpected since a B/SiO_2 catalyst with 0.23 wt. % boron showed 92% total olefin selectivity at 4% propane conversion.[13] The boron content did not change, within the error margin of the experiment, indicating that there was insignificant leaching during reaction. This lack of catalytic activity indicates that the boron species in the zeolite framework are surprisingly not active for propane ODH. As a further control, we performed ODH catalytic testing for a catalyst made by incipient wetness impregnation of boron onto the B-MWW zeolite, denoted B/B-MWW. B/B-MWW was made by a similar procedure as B/SiO_2 (see Supporting Information).[13] The B/B-MWW catalyst (1.3 ± 0.1 wt. %) showed similar catalytic activity to the B/SiO_2 catalyst, with a 90% total olefin selectivity at 5% propane conversion. We have previously shown that B/SiO_2 catalysts contain agglomerated boron species as is likely the case for B/B-MWW. As discussed in detail below, the B-MWW is likely an inactive ODH catalyst because it contains very stable and isolated framework species.

To investigate the source of ODH inactivity in B-MWW, we performed ^1H and ^{11}B MAS SSNMR spectroscopy experiments to directly probe the structure and distribution of boron atoms in the zeolite framework. Prior to all SSNMR experiments, the samples were fully dehydrated and further handled in an inert atmosphere. Direct excitation ^{11}B spin echo MAS SSNMR spectra of pristine B-MWW (fresh) and after 12 hours on stream (spent) were recorded at 11.7 T ($\nu_0(^1H)$ = 500 MHz) with a 10 kHz MAS frequency (Figure 1). ^{11}B SSNMR spectra of fresh and spent B-MWW samples were fit to three sites and display near identical quadrupolar powder patterns, suggesting no boron restructuring occurred under the reaction conditions (Table 1). The ^{11}B isotropic chemical shift (δ_{iso}), electric field gradient asymmetry parameter (η) and quadrupolar coupling constant (C_Q) values are characteristic of trigonal-planar boron species (Figure S2).[12,22,23] The validity of the three site analytical fits in Figure 1 were further confirmed by a 2D ^{11}B triple-quantum multiple-quantum MAS (MQMAS) spectrum of B-MWW fresh, fitting a 9.4 T spin echo ^{11}B SSNMR spectrum (Figure S3) and by performing 2D ^1H-^{11}B heteronuclear correlation (HETCOR) experiments (discussed below). On the basis of $\delta_{iso}(^{11}B)$, the simulated peaks with $\delta_{iso}(^{11}B)$ = 11 ppm (red fit) and $\delta_{iso}(^{11}B)$ = 12 ppm (green fit) are assigned to framework $B(OSi)_3$ species substituted into the zeolite.[12,22-24] The observed distribution in $\delta_{iso}(^{11}B)$ is expected because MWW has eight T-sites that boron could occupy, resulting in a distribution in boron sites from the subtle difference in chemical environment.[24,25] Based upon the analytical simulations, $B(OSi)_3$ units make up ca. 90% of the boron incorporated into the framework. The peak with $\delta_{iso}(^{11}B)$ = 15 ppm and ca. 10% integrated intensity is assigned to a $B(OSi)_2(OH)$ species consisting of two bonds to the framework and a terminal hydroxide. All of these assignments are consistent with the findings of Zones and co-workers who previously used ^1H, ^{11}B and ^{29}Si SSNMR spectroscopy to characterized boron doped B-β, B-SSZ-33 and B-SSZ-42 zeolites.[24] Their high field (19.6 T) ^{11}B spin echo, 2D $^1H \rightarrow ^{11}B$ CP-HETCOR and ^{11}B MQMAS SSNMR spectra clearly showed that $B(OSi)_3$ and $B(OSi)_2(OH)$ incorporated into the framework ($\delta_{iso}(^{11}B)$ = 10.0 – 14.8 ppm, depending on the zeolite) resonate at a lower $\delta_{iso}(^{11}B)$ than non-framework boron species (18.0 ppm).[24] The $\delta_{iso}(^{11}B)$ of $B(OSi)_3$ and $B(OSi)_2(OH)$ species measured by Zones *et. al.* matches our results very well, verifying that B-MWW synthesized here contains primarily framework species.[24]

In comparison, the ^{11}B spin echo spectrum of the active ODH catalyst B/B-MWW reveals that 57 % of the boron species are framework $B(OSi)_3$ groups ($\delta_{iso}(^{11}B)$ = 11 ppm) and 43 % are $B(OSi)_2(OH)$ species ($\delta_{iso}(^{11}B)$ = 15 ppm, Figures S4-S5). Clearly, the $B(OSi)_2(OH)$ sites now make up a larger fraction of the boron species in B/B-MWW. The ^{11}B spin echo spectrum of B/B-MWW and accompanying NMR parameters are similar to that of catalytically active B/SiO_2.[13] While we have assigned the ^{11}B NMR signals of B/B-MWW as framework $B(OSi)_3$ and $B(OSi)_2(OH)$ because of the similarity in ^{11}B NMR parameters to B-MWW, some of the ^{11}B NMR signal from B/B-MWW likely arise from clustered boron sites, as discussed below.

To better understand the boron speciation and confirm the assignments of the distinct ^{11}B NMR signals for B-MWW, we performed ^1H-^{11}B correlation NMR experiments. Because of the similarity in the 1D ^{11}B SSNMR spectra for fresh and spent B-MWW, we only consider the fresh material for these experiments. 2D $^{11}B \rightarrow ^1H$ dipolar-refocused INEPT (D-RINEPT) spectra were recorded with 0.64 ms (blue) or 2.56 ms (red) of total $SR4_1^2$ ^1H heteronuclear dipolar recoupling and a 25 kHz MAS frequency (Figure 2a).[26,27] Analysis of the 1D D-RINEPT and 2D$^{11}B \rightarrow ^1H$ D-RINEPT spectra clearly illustrates that distinct ^1H and ^{11}B resonances can be observed depending on the duration of heteronuclear dipolar recoupling. With 0.64 ms of recoupling (blue trace), only the higher frequency ^1H NMR signals (ca. 3.6 ppm) are observed and they show intense correlations to the higher frequency ^{11}B NMR signal ($\delta_{iso} \approx$ 15 ppm, Figure 2b and Figure S6). On the basis of the chemical shifts, the ^1H NMR signal at 3.6 ppm and ^{11}B NMR signal with δ_{iso} = 15 ppm are assigned to framework $B(OSi)_2(OH)$ species (Figure 3). The 2D $^{11}B \rightarrow ^1H$ D-RINEPT spectrum recorded with 2.56 ms of dipolar recoupling

shows additional strong correlations between the ^{1}H NMR signal at 2.7 ppm and ^{11}B NMR signal with δ_{iso} of 12-11 ppm. Notably, the ^{11}B NMR spectrum extracted from this 2D ^{11}B→^{1}H D-RINEPT spectrum is essentially identical in appearance to the ^{11}B spin echo spectrum (Figure 2b and Figure S6), suggesting that all boron atoms within B-MWW are proximate to ^{1}H spins. In contrast, , the ^{11}B NMR spectrum of B/B-MWW extracted from the 2D D-RINEPT experiment shows different signal intensities from the corresponding ^{11}B spin echo NMR spectrum (Figure S5). Taken together these observations suggest that some boron spins are distant from protons, likely due to the formation of some boron oxide clusters in B/B-MWW.

To estimate the ^{1}H-^{11}B inter-nuclear distance for each pair of ^{1}H-^{11}B NMR signals and thus provide a more detailed structure of boron incorporation into the zeolite framework, we recorded ^{1}H-^{11}B dipolar recoupling build-up curves using the ^{11}B→^{1}H D-RINEPT sequence. In this experiment, the ^{11}B→^{1}H D-RINEPT ^{1}H NMR signal intensity is recorded as a function of the heteronuclear dipolar recoupling duration (Figure 2c and 2d). The dipolar coupling constant (D_{ij}) between two spins is proportional to the inverse of the distance cubed ($D_{ij} \propto r_{ij}^{-3}$). By comparing the experimental build-up curves to numerical SIMPSON simulations for different ^{1}H-^{11}B dipolar coupling constants, ^{1}H-^{11}B inter-nuclear distances can be estimated.[28,29] The D-RINEPT signal build-up for the ^{1}H NMR signal at 3.6 ppm fits best to a simulated curve with a dipolar coupling constant of ca. 3.6 kHz, corresponding to a ^{1}H-^{11}B inter-nuclear distance of ca. 2.2 Å (Figure 2c and Figure S7a). It is important to keep in mind that an H atom in an isolated B-OH group may experience some degree of rotation. Rotation will partially average the ^{1}H-^{11}B dipolar coupling constant, resulting in measurement of lower dipolar coupling constants and longer than expected inter-nuclear distances. The D-RINEPT signal build-up for the ^{1}H NMR signal at 2.7 ppm fits best to a simulated curve with a ^{1}H-^{11}B dipolar coupling constant of ca. 1.6 kHz, corresponding to a 2.9 Å ^{1}H-^{11}B inter-nuclear distance (Figure 2d and Figure S7b). Taking into account the ^{11}B δ_{iso} of 11 ppm and the relatively large ^{1}H-^{11}B inter-nuclear distance, this ^{1}H signal is assigned to a framework $B(OSi)_3$ species that is adjacent to a framework silanol (Figure 3), in agreement with previous models of boron substituted zeolites.[24] A proton detected ^{1}H{^{29}Si} cross polarization MAS (CPMAS) spectrum of fresh B-MWW confirms that the ^{1}H NMR signals at ca. 2.7 ppm results from a silanol defect adjacent to boron (Figure S9).[21,24,30,31] Note that ^{1}H{^{29}Si} CPMAS spectrum of B-MWW fresh required ca. 10 hours of signal averaging, confirming the majority of the zeolite framework is pristine. Infrared spectroscopy of the dehydrated B-MWW confirms that B-OH as well as silanol defect sites are present in the fresh and spent sample (Figure S10).[32]

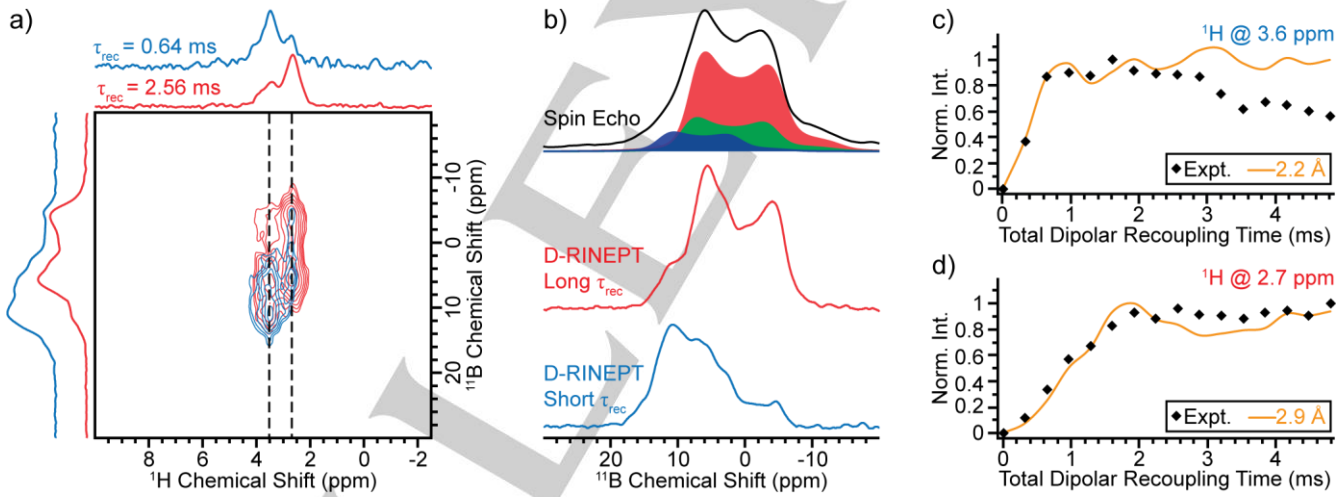

Figure 2. (a) 2D ^{11}B→^{1}H D-RINEPT spectra of B-MWW fresh acquired with 0.64 ms (blue) and 2.56 ms (red) of total $SR4_1^2$ heteronuclear dipolar recoupling. (b) (black) Comparison of 1D ^{11}B spin echo NMR spectrum and projections from the 2D ^{11}B→^{1}H D-RINEPT spectra acquired with 0.64 ms (blue) and 2.56 ms (red) of total heteronuclear dipolar recoupling. (c, d) ^{11}B→^{1}H D-RINEPT dipolar recoupling buildup curves for the ^{1}H slice at (c) 3.6 ppm and (d) 2.7 ppm (dashed black lines in Figure 2a, Figure S8). The black diamonds represent experimental data points and the solid lines correspond to numerical simulations (SIMPSON) for heteronuclear dipolar couplings corresponding to the indicated ^{1}H-^{11}B inter-nuclear distances. The numerically simulated curve with the lowest RMSD is shown, and curves for other coupling strengths are shown in Figure S7. All spectra were recorded at 9.4 T (ν_0(^{1}H) = 400 MHz) with 25 kHz MAS.

In summary, the ^{11}B chemical shifts suggest that in B-MWW nearly all boron atoms are incorporated into the framework. The SSNMR data also suggests that these sites are also well separated (> 3-4 Å apart) from one another, for the reasons given below. In the 2D ^{11}B→^{1}H DRINEPT spectrum of B-MWW recorded with 2.56 ms of recoupling only weak correlations are observed between the $B(OSi)_2(\mathbf{OH})$ ^{1}H NMR signal at 3.6 ppm and the $\mathbf{B}(OSi)_3$ ^{11}B NMR signals, suggesting these sites are well separated within the zeolite. This interpretation is confirmed by a 2D ^{1}H-^{1}H dipolar double quantum-single quantum (DQ-SQ) homonuclear correlation spectrum of B-MWW which shows that the ^{1}H NMR signals at 2.7 ppm, assigned to silanol adjacent to $B(OSi)_3$, do not give rise to any appreciable DQ signal intensity (Figure S11). In comparison, these silanol groups give rise to an observable ^{1}H DQ NMR signal in B/B-MWW, consistent with more extensive aggregation of boron sites in this material. Finally, 1D ^{11}B-^{11}B DQ-SQ experiments show that the DQ-filtered ^{11}B NMR

signal for B-MWW is about three times less than that of B/B-MWW (Figure S12).[33-35] Notably, the DQ-filtered ^{11}B solid-state NMR spectra of B-MWW and B/B-MWW both show signals with more positive chemical shifts as compared to the SQ ^{11}B spin echo spectra. The more positive shifts suggest that aggregation preferentially occurs for hydroxylated or oxide-like boron sites, both of which are much more common in B/B-MWW as shown by quantitative ^{11}B spin echo experiments above. All of these observations confirm the hypothesis that catalytically inactive B-MWW consist of predominately isolated boron sites incorporated into the zeolite framework, while the active ODH catalyst B/B-MWW contains some partially aggregated boron sites.

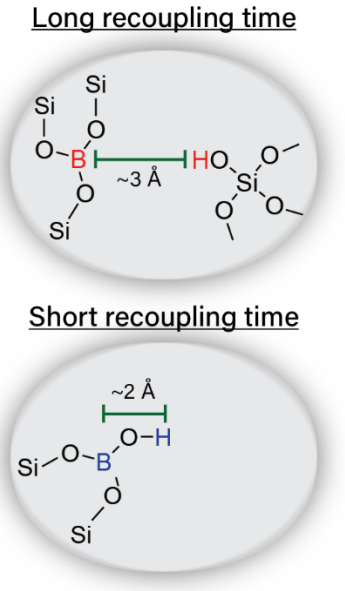

Figure 3. Simplified illustration of the two different ^{1}H-^{11}B interactions observed in the 2D ^{11}B→^{1}H D-RINEPT spectra and molecular structures of framework boron sites.

In this work, we successfully synthesized stable, isolated framework $B(OSi)_3$ (major, ca. 90 %) and $B(OSi)_2(OH)$ (minor, ca. 10 %) species in zeolite MWW framework and catalytically tested them for the ODH of propane. The detailed characterization of B-MWW by multi-dimensional ^{1}H and ^{11}B SSNMR spectroscopy showed that boron exists predominantly as isolated $B(OSi)_3$ units that are adjacent to a silanol group. Although B-MWW has a boron loading sufficient for catalytic activity, testing determined that it did not exhibit any ODH conversion of propane over background levels. As was shown here and in our prior work, catalytically active B/B-MWW, B/SiO_2 and boron nitride ODH catalysts contain aggregated boron sites that restructure under reaction conditions, whereas B-MWW is stable under reaction conditions and shows no restructuring of the boron atoms.[12,13] The difference in boron sites in B-MWW and these other boron materials leads us to the important conclusion that the boron-catalyzed ODH of propane does not proceed over an isolated BO_3 site. Rather, active boron-based ODH catalysts likely requires boron species with some degree of B-O-B connectivity. This study advances the understanding of boron species involved in the propane ODH mechanism and will direct future work in understanding the molecular origins of highly selective ODH catalysts. Further investigations are underway to determine the surface mobility and understand precisely which types of boron-boron interactions are required to form active ODH catalysts.

Supporting Information: Additional characterization and experimental details are available in the Supporting Information. doi: 10.1002/anie.201914696

Acknowledgements

Materials synthesis and characterization was supported by the National Science Foundation under Grant No. CBET-1916809. Catalytic testing was supported by the U.S. Department of Energy under Grant No. DE-SC0017918. A.J.R. also thanks the Ames Laboratory Royalty Account and Iowa State University for additional funding. The Ames Laboratory is operated for the U.S. DOE by Iowa State University under Contract No. DE-AC02-07CH11358. This study made use of the National Magnetic Resonance Facility at Madison, which is supported by NIH grants P41 GM103399 (NIGMS) and P41GM66326 (NIGMS). Additional equipment was purchased with funds from the University of Wisconsin, the NIH (RR02781, RR08438), the NSF (DMB-8415048, OIA-9977486, BIR-9214394), and the USDA. We thank Prof. Aaron Sadow (ISU and Ames lab) for access to a glovebox to pack and store rotors.

Keywords: zeolites • boron • heterogeneous catalysis • oxidative dehydrogenation • solid-state NMR

[1] B. Yilmaz, U. Müller, in *Top. Catal.*, **2009**, pp. 888–895.
[2] W.M.H. Sachtler, Z. Zhang, Adv. Catal. **1993**, 39, 129–220.
[3] P. Wolf, M. Valla, A.J. Rossini, A. Comas-Vives, F. Núñez-Zarur, B. Malaman, A. Lesage, L. Emsley, C. Copéret, I. Hermans, *Angew. Chemie - Int. Ed.* **2014**, *53*, 10179–10183.
[4] M. Shamzhy, M. Opanasenko, P. Concepción, A. Martínez, *Chem. Soc. Rev.* **2019**, *48*, 1095–1149.
[5] J.T. Grant, C. A. Carrero, F. Goeltl, J. Venegas, P. Mueller, S.P. Burt, S. E. Specht, W. P. McDermott, A. Chieregato, I. Hermans, *Science.* **2016**, *354*, 1570–1573.
[6] F. Guo, P. Yang, Z. Pan, X.N. Cao, Z. Xie, X. Wang, *Angew. Chemie - Int. Ed.* **2017**, *56*, 8231–8235.
[7] R. Huang, B. Zhang, J. Wang, K.H. Wu, W. Shi, Y. Zhang, Y. Liu, A. Zheng, R. Schlögl, D. S. Su, *ChemCatChem* **2017**, *9*, 3293–3297.
[8] L. Shi, D. Wang, W. Song, D. Shao, W.P. Zhang, A.H. Lu, *ChemCatChem* **2017**, *9*, 1720.
[9] L. Shi, B. Yan, D. Shao, F. Jiang, D. Wang, A.H. Lu, *Cuihua Xuebao/Chinese J. Catal.* **2017**, *38*, 389–395.
[10] J.M. Venegas, J.T. Grant, W.P. McDermott, S.P. Burt, J. Micka, C.A. Carrero, I. Hermans, *ChemCatChem* **2017**, *9*, 2118–2127.
[11] J.T. Grant, W.P. McDermott, J.M. Venegas, S.P. Burt, J. Micka, S.P. Phivilay, C.A. Carrero, I. Hermans, *ChemCatChem* **2017**, *9*, 3622.
[12] A.M. Love, B. Thomas, S.E. Specht, M.P. Hanrahan, J.M. Venegas, S.P. Burt, J.T. Grant, M.C. Cendejas, W.P. McDermott, A.J. Rossini, et al., *J. Am. Chem. Soc.* **2019**, *141*, 182–190.
[13] A.M. Love, M.C. Cendejas, B. Thomas, W.P. McDermott, P. Uchupalanun, C. Kruszynski, S.P. Burt, T. Agbi, A.J. Rossini, I. Hermans, *J. Phys. Chem. C* **2019**, acs.jpcc.9b07429.
[14] Z. Zhang, E. Jimenez-Izal, I. Hermans, A.N. Alexandrova, *J. Phys. Chem. Lett.* **2019**, *10*, 20–25.

[15] A. Corma, J. Martínez-Triguero, *J. Catal.* **1997**, *165*, 102–120.
[16] J.C. Cheng, A.S. Fung, D.J. Klocke, L.S. L., D.N. Lissy, W.J. Roth, C.M. Smith, D.E. Walsh, *US5453554A*, **2011**, 585/467.
[17] J. Rigoreau, S. Laforge, N. S. Gnep, M. Guisnet, *J. Catal.* **2005**, *236*, 45–54.
[18] F. Song, Y. Liu, L. Wang, H. Zhang, M. He, P. Wu, in *Stud. Surf. Sci. Catal.*, Elsevier Inc., **2007**, pp. 1236–1243.
[19] L. Liu, M. Cheng, D. Ma, G. Hu, X. Pan, X. Bao, *Microporous Mesoporous Mater.* **2006**, *94*, 304–312.
[20] L. Ren, Q. Guo, M. Orazov, D. Xu, D. Politi, P. Kumar, S.M. Alhassan, K.A. Mkhoyan, D. Sidiras, M.E. Davis, et al., *ChemCatChem* **2016**, *8*, 1274–1278.
[21] J. Chen, T. Liang, J. Li, S. Wang, Z. Qin, P. Wang, L. Huang, W. Fan, J. Wang, *ACS Catal.* **2016**, *6*, 2299–2313.
[22] S. Kroeker, J. F. Stebbins, *Inorg. Chem.* **2001**, *40*, 6239–6246.
[23] Y.T. Angel Wong, D.L. Bryce, in *Annu. Reports NMR Spectrosc.*, **2018**, *93*, 213–279.
[24] S.J. Hwang, C.Y. Chen, S.I. Zones, *J. Phys. Chem. B* **2004**, *108*, 18535–18546.
[25] M.E. Leonowicz, J.A. Lawton, S.L. Lawton, M.K. Rubin, *Science*, **1994**, *264*, 1910-1913.
[26] J. Trebosc, B. Hu, J.P. Amoureux, Z. Gan, *J. Magn. Reson.* **2007**, *186*, 220–227.
[27] A. Venkatesh, M.P. Hanrahan, A.J. Rossini, *Solid State Nucl. Magn. Reson.* **2017**, *84*, 171–181.
[28] Z. Tošner, R. Andersen, B. Stevensson, M. Edén, N.C. Nielsen, T. Vosegaard, *J. Magn. Reson.* **2014**, *246*, 79–93.
[29] M. Bak, J.T. Rasmussen, N.C. Nielsen, *J. Magn. Reson.* **2000**, *147*, 296–330.
[30] K.F.M.G.J. Scholle, W.S. Veeman, *Zeolites* **1985**, *5*, 118–122.
[31] R. de Ruiter, A.P. M. Kentgens, J. Grootendorst, J.C. Jansen, H. van Bekkum, *Zeolites* **1993**, *13*, 128–138.
[32] H. Robson, "Verified Synthesis of Zeolitic Materials: Second Edition," **2001**.
[33] M. Edén, D. Zhou, J. Yu, *Chem. Phys. Lett.* **2006**, *431*, 397–403.
[34] Q. Wang, B. Hu, O. Lafon, J. Trébosc, F. Deng, J. P. Amoureux, *J. Magn. Reson.* **2009**, *200*, 251–260.
[35] G. Mali, G. Fink, F. Taulelle, *J. Chem. Phys.* **2004**, *120*, 2835–2845.

COMMUNICATION

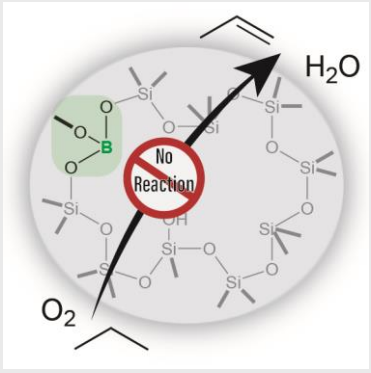

Natalie R. Altvater[‡][a], Rick W. Dorn[‡][b][c], Melissa C. Cendejas[‡][d], William P. McDermott[d], Brijith Thomas[b], Aaron J. Rossini[*][b][c], Ive Hermans[*][a][d]

Page No. – Page No.

B-MWW Zeolite: The Case Against Single-Site Catalysis

Detailed solid-state NMR spectroscopic characterization of hydrothermally synthesized B-MWW reveals that boron is fully incorporated into the zeolite framework as trivalent BO_3 units. These isolated sites are inactive for oxidative dehydrogenation (ODH) of propane, which refutes the hypothesis that site-isolated boron species are the active site on boron-containing ODH catalysts.